Eurasian J. Sci. Eng. Tech., 2025; 6(1): 036-040

Eurasian Journal of Science Engineering and Technology

Research article

www.dergipark.org.tr/tr/pub/ejset / www.dergipark.org.tr/en/pub/ejset

Enhancing optoelectronic performance: Structural and optical properties of MZO thin films

Ali Altuntepe [1,*], Serkan Erkan [2]

[1] *Sivas of Science and Technology University Optical Excellence Application and Research Center, 58000, Sivas, Türkiye*
[2] *Nigde Omer Halisdemir University, Nanotechnology Research and Application Center, 51240, Niğde, Türkiye*

Abstract

This work reports on the feasibility of using molybdenum-doped zinc oxide (MZO) thin films as transparent conductive electrode (TCE) material in optoelectronic applications, especially in solar cells. MZO films were deposited by RF magnetron sputtering in the thickness range of 100-500 nm and their electrical, optical, and structural properties were systematically studied. The results indicated that the electrical conductivity increased with the increase in film thickness, while the sheet resistance decreased; the 500 nm MZO film had the least resistance, which was about 362.4 Ω/sq. The optical measurements presented an average transmittance of about 77–84% in the visible range, with minor variations attributed to graphene integration in hybrid MZO+Graphene structures. The bandgap energy of MZO films decreased from 3.29 eV to 3.21 eV with increasing thickness, indicating the transition from quantum confinement toward bulk-like properties. SEM and EDXS analyses confirmed successful doping with molybdenum and gave insight into the surface morphology and chemical composition of the films. While MZO films with improved electrical and optical performances were reported when compared to undoped zinc oxide (ZnO), the hybrid structures showed a high sheet resistance due to inherent characteristics of graphene. The presented work demonstrates the MZO films as potential alternatives for more conventional TCE materials like indium tin oxide (ITO), considering their cost and availability issues, as well as their structure-related shortcomings.

Keywords: MZO, Magnetron sputtering, Pressure, Graphene

1 Introduction

In silicon-based solar cells, one of the primary cost-increasing factors is the amount of material used (~180 µm). The main reason thin-film technology is widely studied is the significantly reduced material usage (2–10 µm) compared to Si-based solar cells. Another major cost factor in Si-based solar cells is the transparent conductive electrode (TCE) material, indium tin oxide (ITO) [1]. ITO thin films exhibit low thickness and sheet resistance while maintaining high optical transparency in the visible region. Despite its advantages, ITO has some inherent issues. The main drawbacks include the lack of a uniform crystalline structure and a high density of structural defects. In its amorphous form, substitutional reactions between +3 valence indium and +4 valence tin do not occur, and the film structure contains high levels of impurities. Consequently, the carrier density and mobility remain quite low, which significantly limits cell efficiency (Mazur vd., 2010). In addition to ITO, zinc oxide-based TCEs are used to a limited extent. Structural defects and high sheet resistance in zinc oxide (ZnO) require various structural enhancement methods for solar cell applications. Chemical doping has facilitated the use of ZnO-based TCEs in such applications. Aluminum-doped zinc oxide (AZO), molybdenum-doped zinc oxide (MZO), and gallium-doped zinc oxide (GZO) are particularly employed in optoelectronic applications such as sensors, transistors, and thin-film solar cells [2-5].

Molybdenum (Mo)-doped ZnO (MZO) films have recently emerged as popular TCE materials. Like gallium, molybdenum enables stable doping due to its ionic radius (0.062 nm), which is close to that of Zn. Molybdenum, in its 4+ or 6+ oxidation states, integrates into the Zn structure and contributes two or four electrons to ZnO's conduction band, thereby enhancing electrical conductivity. Studies on MZO films report resistivity values in the range of approximately 10−3-10−4 ohm-cm [6]. Despite these promising features, MZO films also present challenges, primarily low oxidation resistance [7]. Moreover, the electrical properties of MZO films can vary depending on the production method. Research continues on parameters such as doping ratios, temperature effects, and film thickness in MZO structures [8, 9]. In general, the disadvantages of TCEs include structural defects and the limited carrier density at similar levels. To address these issues, graphene—a carbon-based material often referred to as a "miracle material"—stands out as one of the best candidates. Graphene, defined as the first two-dimensional material synthesized with a hexagonal honeycomb lattice, was isolated in 2004 by Novoselov and colleagues using mechanical exfoliation. It quickly became a focus of interest due to its exceptional properties, including high strength (1 TPa Young's modulus), excellent electrical conductivity, and high optical transparency (97%). These combined properties make graphene applicable in a wide range of fields [10]. Graphene is utilized in solar cells, fuel cells, sensors, transistors, and many other electronic and

* Corresponding author, e-mail: altuntepeali@gmail.com (A. Altuntepe)
Recieved: 20.12.2024 Accepted: 09.01.2025 Published: 30.01.2025
doi: 10.55696/ejset.1604813

optoelectronic applications. Notably, it offers a strong alternative to ITO, which is commonly used as a transparent conductive electrode in solar cells [11]. The brittle nature of ITO, its limited natural reserves, and its significantly lower carrier density compared to graphene highlight the importance of integrating graphene as a TCE. In summary, while the growth parameters for MZO have been optimized, this study presents research on hybrid TCEs combining graphene.

2 Material and method

All films were deposited using an RF power source and a single target. Before initiating the deposition process, the sputtering system was evacuated to a pressure below $1.6x10^{-6}$ Torr after placing the substrates. High-purity argon (Ar, 99.999%) gas was then introduced into the system to generate the plasma required for sputtering, preparing the system for the deposition process. Each TCE film was deposited by applying 50 W of power. MZO films with thicknesses of 100, 200, 300, 400, and 500 nm were deposited on glass substrates. This approach allowed the investigation of the effect of film thickness on the electrical and optical properties of the TCE layer. The CVD system used for graphene synthesis comprises three zones and six gas flow control units. Polycrystalline copper substrates with a thickness of 25 µm were utilized, sourced from Alfa Easer. Methane (CH_4, 99.9995% purity) served as the carbon source, while hydrogen (H_2, 99.9999% purity) acted as the decomposition agent. The gas flow parameters for single-layer graphene synthesis were previously optimized in our studies [12]. To transfer graphene from the metal substrate to a desired surface, the "wet transfer" method, which employs a polymer support, was used. Initially, the graphene on the copper substrate was coated with poly(methyl methacrylate) (PMMA) using a spin-coating device to protect its surface. The copper substrate was then dissolved in an ammonium persulfate ($(NH_4)_2S_2O_8$) solution, releasing the graphene+polymer structure from the metal surface. This structure was rinsed multiple times in deionized water baths to remove residual impurities. The graphene was subsequently transferred onto a chosen substrate. After the transfer, the substrate was heated on a hot plate at approximately 50-60°C for 3 minutes to remove excess water from the structure, followed by heating at 80°C for 5 minutes. Finally, the polymer layer used during the transfer process was removed from the graphene surface using acetone.

Table 1. Growth process of MZO

Growth Process	
Base Pressure	$1.6x10^{-6}$ Torr
Growth Pressure	$3x10^{-3}$ Torr
RF Power	50 Watt
Deposition Rate	0.2 Å/s
Temperature	RT

3 Results and discussion

MZO films were growth at varying thicknesses (100–500 nm). A significant factor in the improved electrical properties of MZO films compared to ZnO is the four-valence difference between Mo^{6+} and Zn^{2+}. The presence of Mo as a dopant contributes additional electrons to electrical conductivity, enhancing the electrical properties of ZnO-based MZO films and making them suitable for TCE applications. Sheet resistance measurements of MZO+Graphene films showed an increase in resistance compared to MZO films alone (Table 2). Similar to AZO films, the sheet resistance of MZO films being higher or comparable to that of graphene leads to an increase in the overall sheet resistance of the MZO+Graphene structure. Despite this, the decrease in sheet resistance with increasing MZO film thickness was also observed in MZO+Graphene films. The measurements revealed that MZO films have lower sheet resistance compared to AZO films. This indicates that different dopants significantly influence the electrical properties of ZnO-based films. As the film thickness increases, the sheet resistance of MZO films decreases, which is accompanied by an improvement in crystal quality. This contributes to an increase in carrier concentration, thereby enhancing the electrical properties [13]. For example, a 100 nm MZO film exhibits a sheet resistance of 819 ohm/sq, while a 500 nm MZO film has a resistance of 362 ohm/sq. The sheet resistance continued to decrease for films of all thicknesses up to 500 nm.

Table 2. The sheet resistance, optical transmission, and bandgap values of MZO films.

			MZO		
	MZO	**MZO+Graphene**	**MZO**	**MZO+Graphene**	**MZO**
Thickness (nm)	**Sheet Resistance (ohm/sq)**	**Sheet Resistance (ohm/sq)**	**Transmission (%)**	**Transmission (%)**	**E_g (eV)**
100	751.98	1051	81	83	3.29
200	643.26	843.6	79	81	3.28
300	588.9	730	78	78	3.27
400	498.3	589.8	80	76	3.24
500	362.4	434.2	80	80	3.21

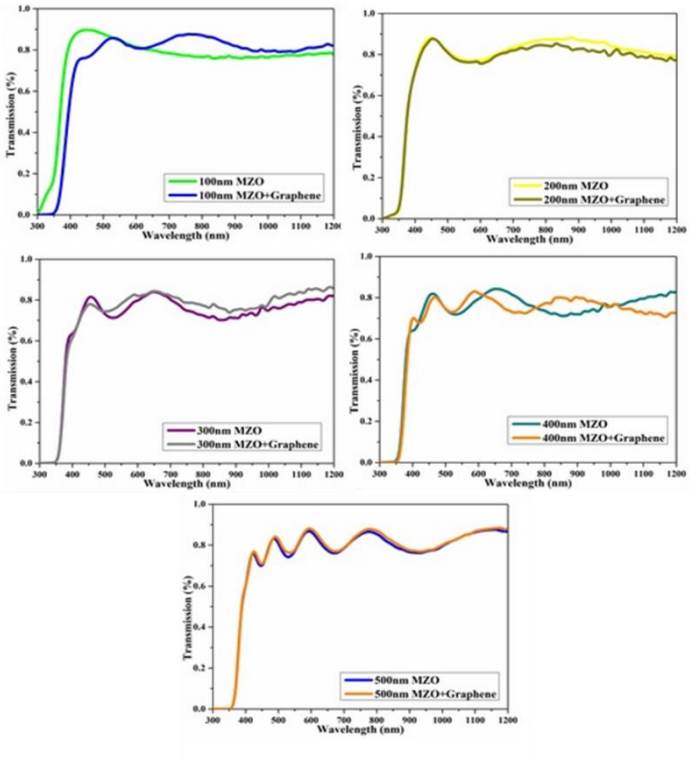

Figure 1. The optical transmission values of MZO and MZO+Graphene films.

MZO films exhibit average optical transmittance values ranging between 77% and 84% in the visible region. It is observed that graphene coating causes partial increases and decreases in transmittance values; however, these variations are considered within the margin of error. Nevertheless, in MZO+Graphene films, an improvement in optical transmittance values was generally noted beyond a wavelength of 700 nm. This can be attributed to the material used in the hybrid TCE structure being graphene. Graphene's low absorption values beyond 700 nm contribute positively to the optical transmittance values in the hybrid structures. The band gap is an important characteristic of semiconductors, and it determines their electrical and optical properties. The optical properties of the MZO films growth on glass substrate were determined by using the bandgap values calculated from the absorption coefficient obtained by the transmittance spectra of the samples. The bandgap energy values of the samples were calculated by measuring the transmittance spectra with an ellipsometer (J.A. Woollam-VASE) system in our research center. The absorption coefficients of the samples were calculated using the Lambert-Beer law [14] with the measured transmittance values at room temperature in the range of 200-1200 nm and the thicknesses of the MZO films.

$$\alpha = \frac{1}{d}\ln\frac{1}{T} \quad (1)$$

The absorption coefficient (α) in Equation (1) represents the absorption coefficient, d represents the thickness of the sample, and T represents the optical transmittance. Using the calculated absorption coefficients with Equation (1), the bandgap energy values of the MZO films were calculated using Equation (2), where E_g is the bandgap energy, A is the constant, $h\nu$ is the photon energy, and n is the nature of the transition, which takes the value of 1/2 for direct bandgap semiconductors [15].

$$(\alpha h\nu)^2 = A(h\nu - E_g)^n \quad (2)$$

The optical band gap MZO films shows a slight decreasing trend as the film thickness increases. At 100 nm, the band gap is 3.29 eV, and as the thickness increases, it gradually decreases, reaching 3.21 eV at 500 nm. This reduction in band gap can be attributed to several factors. First, in very thin films, quantum confinement effects are more pronounced, which leads to a wider band gap. As the film thickness increases, these quantum effects diminish, allowing the material to approach bulk-like properties where the band gap is generally smaller. Additionally, thicker films tend to have fewer strain effects, as they may relax more compared to thinner films, which can contribute to a slight narrowing of the band gap. The defect density, often higher in thinner films, can also lead to localized states within the band gap, which reduces as the film thickens, resulting in a more stable electronic structure and a smaller band gap. This behavior reflects the transition from quantum confinement to bulk-like properties, which is typical for semiconductor thin films. As shown in the Figure 2, graphene coating does not appear to have an impact on the bandgap energy. An observed decrease in bandgap energy occurs with increasing

film thickness (Table 1). Similarly, studies in the literature have also demonstrated the effect of film thickness on bandgap energy [16-17]. Fundamentally, with increasing film thickness, grain boundaries expand, and the crystal structure improves accordingly. This can be correlated with the changes observed in the bandgap energy.

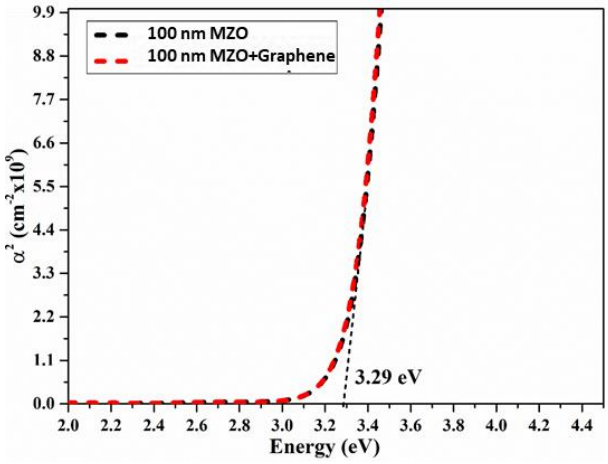

Figure 2. Band gap for the 100 nm MZO film.

The SEM and EDXS measurements of the optimized thickness MZO films have been performed (Table 2). Based on the obtained SEM-EDXS results, information regarding the surface microstructures and chemical compositions of the films has been gathered. These techniques provide valuable insights into the morphology, grain size, surface uniformity, and the distribution of elements within the films. SEM imaging helps to visualize the surface structure, while EDXS analysis allows for the precise determination of the elemental composition, confirming the successful doping of molybdenum and the overall material consistency. This analysis is crucial for understanding the relationship between the film's structural characteristics and its electrical and optical properties. It has been observed that the presence of Mo atoms within the structure of MZO films is at a very low level. This can be explained by either the inability of Mo atoms to incorporate into the structure during sputtering or the lack of sufficient sensitivity in the EDXS measurements.

Table 3. Chemical compositions of MZO film.

TCE	Atomic Ratio (%)		
	O	Zn	Mo
100nm MZO	62.55	37.37	0.08

The SEM surface images of the 100 nm MZO film are shown in Figure 3, providing insights into the morphological characteristics of the film. As observed, the surface exhibits a uniform and dense structure, indicating good coverage and homogeneity. This suggests that the deposition process resulted in a consistent film formation without significant defects or irregularities.

However, the grain boundaries in the SEM images appear less defined, and the individual grains are not prominently visible. This can be attributed to two primary factors. First, the relatively low thickness of the film (100 nm) limits the growth of larger grains, as thinner films typically have smaller grain sizes due to the limited material available for crystallization. Second, the absence of thermal treatment, such as annealing, prevents further recrystallization and grain growth. Thermal processes are known to enhance grain boundary mobility, allowing grains to coalesce and grow, leading to a more distinct grain structure.

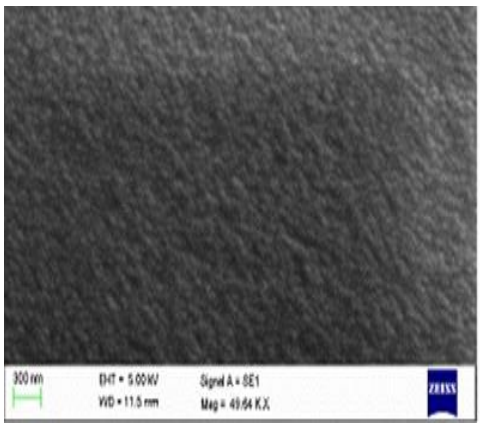

Figure 3. SEM surface images of MZO thin film

When the electrical and optical properties of MZO films were examined, it was determined that 050 nm MZO film exhibited better properties compared to other films. In this sense, it was determined that the most suitable film thickness for MZO films to be used as TCE in solar cell applications was 100 nm.

4 Conclusion

MZO films showed enhanced electrical and optical properties with increasing film thickness, such as lower sheet resistance, higher carrier concentration, and better crystal quality. The reduction in bandgap energy with increasing film thickness was explained by quantum confinement effects and structural improvements. The incorporation of graphene into MZO structures led to significant changes in optical transmittance, especially in the near-infrared region. Although the addition of graphene slightly increased sheet resistance compared to pure MZO films, its low absorption characteristics enhanced optical transmittance beyond 700 nm. This suggests the synergistic possibility of hybrid TCE structures in applications that demand both high transparency and electrical conductivity.

The study also underlines the importance of optimizing parameters related to film thickness, doping levels, and deposition methods for achieving maximum performance. Notwithstanding the challenges in achieving uniform Mo doping, besides variability in electrical properties arising out of production methods, MZO+Graphene structures present an encouraging alternative to traditional TCEs like ITO. More research is required for addressing the challenges, refining the fabrication techniques, and exploring scalability for industrial applications. This will help develop further understanding of hybrid TCEs and create pathways for their incorporation into next-generation optoelectronic devices,

such as solar cells, for which issues of cost, efficiency, and material sustainability will remain pressing.

Conflict of interest

The authors declare that there is no conflict of interest.

Similarity rate (iThenticate): .15 %

References

[1] A. M. Bagher, M. M. A. Vahid, and M. J. Mohsen, "Types of solar cells and application," *Photonics*, vol. 3, no. 2, pp. 94–113, 2015, doi: 10.1515/pn-2015-0005.

[2] S.-W. Ko, J.-G. Jung, K.-S. Park, and S.-M. Lim, "Adhesion change of AZO/PET film by ZrCu insertion layer," *J. Korean Phys. Soc.*, vol. 49, no. 2, pp. 252–259, 2016, doi: 10.1007/s00339-015-9459-4.

[3] G. Gonçalves, E. Elangovan, P. Barquinha, L. Pereira, R. Martins, and E. Fortunato, "Influence of post-annealing temperature on the properties exhibited by ITO, IZO and GZO thin films," *Thin Solid Films*, vol. 515, no. 22, pp. 8562–8566, Sep. 2007, doi: 10.1016/j.tsf.2007.03.034.

[4] F. Bittau et al., "Analysis and optimisation of the glass/TCO/MZO stack for thin film CdTe solar cells," *Sol. Energy Mater. Sol. Cells*, vol. 187, pp. 15–22, Sep. 2018, doi: 10.1016/j.solmat.2018.07.001.

[5] K. Girija et al., "Enhanced H_2S sensing properties of gallium doped ZnO nanocrystalline films as investigated by DC conductivity and impedance spectroscopy," *Mater. Chem. Phys.*, vol. 214, pp. 297–305, Jul. 2018, doi: 10.1016/j.matchemphys.2018.04.063.

[6] S. Zhang, S.-H. Wei, and A. Zunger, "Intrinsic n-type versus p-type doping asymmetry and the defect physics of ZnO," *Phys. Rev. B*, vol. 63, no. 7, p. 075205, Feb. 2001, doi: 10.1103/PhysRevB.63.075205.

[7] C. Wu et al., "Electrical and optical properties of molybdenum-doped ZnO transparent conductive thin films prepared by dc reactive magnetron sputtering," *Semicond. Sci. Technol.*, vol. 24, no. 12, p. 125012, Dec. 2009, doi: 10.1088/0268-1242/24/12/125012.

[8] A. Ali et al., "Mo-doped ZnO nanoflakes on Ni-foam for asymmetric supercapacitor applications," *RSC Adv.*, vol. 9, pp. 27432–27438, 2019, doi: 10.1039/C9RA05046A.

[9] J.-Y. Chun, J.-W. Han, and D.-S. Seo, "Molybdenum-doped zinc oxide electrodes for organic light-emitting devices," *Electron. Lett.*, vol. 45, no. 12, pp. 604–606, 2009, doi: 10.1049/el.2009.0200.

[10] A. K. Geim and K. S. Novoselov, "The rise of graphene," *Nanoscience and Technology: A Collection of Reviews from Nature Journals*, pp. 11–19, 2010, doi: 10.1142/9789814287005_0002.

[11] P. Avouris and F. Xia, "Graphene applications in electronics and photonics," *Mater. Today*, vol. 15, no. 3, pp. 122–130, Mar. 2012, doi: 10.1016/S1369-7021(12)70058-3.

[12] R. Zan et al., "Integration of graphene with GZO as TCO layer and its impact on solar cell performance," *Renew. Energy*, vol. 173, pp. 45–52, 2021, doi: 10.1016/j.renene.2021.03.001.

[13] R. Swapna et al., "Microstructural, electrical and optical properties of ZnO: Mo thin films with various thickness by spray pyrolysis," *J. Alloys Compd.*, vol. 553, pp. 68–75, Jun. 2013, doi: 10.1016/j.jallcom.2012.03.100.

[14] J. I. Pankove, *Optical Processes in Semiconductors*. New York, NY, USA: Dover, 1971.

[15] J. Tauc, "Optical properties and electronic structure of amorphous Ge and Si," *Mater. Res. Bull.*, vol. 3, no. 1, pp. 37–46, 1968, doi: 10.1016/0025-5408(68)90023-8.

[16] X. Xiu et al., "Transparent conducting molybdenum-doped zinc oxide films deposited by RF magnetron sputtering," *Appl. Surf. Sci.*, vol. 253, no. 8, pp. 3345–3348, Feb. 2007, doi: 10.1016/j.apsusc.2006.07.106.

[17] R. Zan, A. Altuntepe, and S. Erkan, "Substitutional boron doping of graphene using diborane in CVD," *Phys. E*, vol. 128, p. 114629, Mar. 2021, doi: 10.1016/j.physe.2021.114629.